

Nanostructured corrosion sensing coatings for aeronautical applications

T.L.P. Galvão
CICECO-Aveiro Institute of Materials, DEMaC
University of Aveiro
Campus de Santiago
Aveiro, 3810-193
Portugal

I. Sousa
CICECO-Aveiro Institute of Materials, DEMaC
University of Aveiro
Campus de Santiago
Aveiro, 3810-193
Portugal

M. Wilhelm
CICECO-Aveiro Institute of Materials, DEMaC
University of Aveiro
Campus de Santiago
Aveiro, 3810-193
Portugal

J. Opršal
SYNPO
S. K. Neumanna
1316, 532 07 Pardubice
Czech Republic

H. Kukačková
SYNPO
S. K. Neumanna
1316, 532 07 Pardubice
Czech Republic

V. Špaček
SYNPO
S. K. Neumanna
1316, 532 07 Pardubice
Czech Republic

N. Scharnagl
Helmholtz-Zentrum Geesthacht Centre for
Materials and Coastal Research GmbH Institute
of Materials Research – MagIC
Max-Planck-Strasse 1
21502 Geesthacht
Germany

F. Maia
Smallmatek, Small Materials and Technologies
Rua dos Canhas
3810-075 Aveiro
Portugal

J. R. B. Gomes
CICECO-Aveiro Institute of Materials, DEMaC
University of Aveiro
Campus de Santiago
Aveiro, 3810-193
Portugal

M. G. S. Ferreira
CICECO-Aveiro Institute of Materials, DEMaC
University of Aveiro
Campus de Santiago
Aveiro, 3810-193
Portugal

João Tedim
CICECO-Aveiro Institute of Materials, DEMaC
University of Aveiro
Campus de Santiago
Aveiro, 3810-193
Portugal

ABSTRACT

It is critical for the aeronautical industry that the next generation of smart coatings allows the early detection and continuous monitoring of corrosion. Once corrosion is detected, preventive actions can be taken in order to mitigate its costs.

Our strategy relies on functional coatings capable of detecting metallic corrosion early on. After appropriate selection of sensing compounds and subsequent loading into nanostructured materials [2], these are incorporated into coating formulations giving them corrosion sensing functionality. Based on this concept we focused on the compatibility between nanocontainers and coating formulations. Thus, a new sensing coating was investigated using immersion and salt-spray tests, release and leaching studies, viscoelastic properties, curing, thermal stability, hardness, mechanical properties and corrosion resistance. The results embody a new generation of coatings with sensing ability, and have implications for self-healing and anti-fouling coatings as well.

Key words: Corrosion, sensors, coatings, pH indicator molecules, silica nanocapsules, controlled release.

INTRODUCTION

Corrosion is a chemical force with an economic impact to be reckoned with. Early detection and subsequent mitigation are fundamental to minimize its costs and propel healthier economies.

Direct impregnation of pH indicators into coatings was a foundational technology that showed the potential to achieve corrosion sensing [1-3]. These functional coatings are capable of changing color when corrosion ensues and pH changes [4].

State of the art technologies rely on the use of hosting structures for detection of corrosion [5] that are able to store pH indicating molecules and release them as active components upon demand. These technologies use micro- and nanomaterials with the capacity to release sensing species upon demand following an external chemical trigger, and can be applied as functional additives for polymeric coatings imparting them self-sensing capability. The advantage of using functional additives instead of directly adding organic compounds to the coatings is to limit detrimental reactions between the compounds and the coating formulation, as well as a more localized response since only materials close to corroded sites will provide a signal.

The solution presented herein revisits and improves previous reports of nanostructured coatings containing silica nanocapsules with phenolphthalein encapsulated [5]. Silica nanoparticles are easy to prepare, have high surface areas, tunable pore sizes and their hollow core allows them to store functional molecules [6,7]. They have grown into one of the structures of choice to design functional materials for different applications [8,9], such as catalysis, adsorption/separation, sensing and active materials.

In the present work, SiNC-PhPh were incorporated into a water borne high-performance lacquer and the new coating was submitted to functionality and standard performance tests.

EXPERIMENTAL PROCEDURE

Synthesis of silica nanocapsules

Silica nanocapsules containing phenolphthalein (SiNC-PhPh) were synthesized according to a procedure reported in literature [10]. An oil-in-water miniemulsion method was employed, with ethyl ether and water, respectively, as the oil and water phases, hexadecyltrimethylammonium bromide (CTAB) as a surfactant, and tetraethyl orthosilicate (TEOS) as the silica precursor.

Coating preparation

After synthesis, SiNC-PhPh were thoroughly washed with water and dispersed in the main component of a water borne lacquer (080) by magnetic stirring for 24 h. The investigated coatings corresponded to 080 with 3 % of dispersed SiNC-PhPh capsules (080-SiNC-PhPh). For comparison, PhPh was also dispersed directly on the polymeric matrix in a proportion corresponding to the encapsulated amount in the capsules (0.3 %, 080-PhPh).

The prepared systems were mixed with the corresponding hardeners. The films were applied on polyethylene and AA2024 substrates using a film applicator with a gap of 150 μm , as represented in Figure 1.

The films were then submitted to the curing process of 24 hours at room temperature and one hour at 100°C. Due to the loss of water during the curing process, the final thickness of the cured coating was around 30 μm .



Figure 1. Film application on a metal.

Characterization techniques

To verify if SiNC-PhPh are functional when present in cured coatings, the respective free films were immersed in an aqueous solution with pH 11. The change of color was analyzed as a function of time.

Coated aluminum alloys 2024 plates were submitted to accelerated corrosion tests. Immersion tests were performed in a 5 % NaCl solution, and salt-spray tests were performed at $T = (35 \pm 2) ^\circ\text{C}$, an average collection rate for a horizontal collecting area of 80 cm^2 of $(1.5 \pm 0.5) \text{ ml}\cdot\text{h}^{-1}$, a NaCl concentration of $(50 \pm 5) \text{ g}\cdot\text{L}^{-1}$, and a pH of 6.5 – 7.2, with an X scribe made on the coated plates to accelerate corrosion and hence coatings response.

A rheometer, with a 4° cone geometry of 40 mm diameter and a gap of 150 μm , at $T = 298\text{ K}$, was used in the rheological study of the formulations.

Differential scanning calorimetry (DSC) was used to study the temperatures of glass transition (T_g) of several cured coating formulations. Thermogravimetric analysis (TG/DTA), under air atmosphere, was used in the study of the thermal stability of the coatings.

Size exclusion chromatography (SEC) experiments were made to verify if PhPh reacted with isocyanates of the coatings. The final product was also analyzed by FT-IR absorbance spectroscopy.

The leaching of PhPh from coatings was followed by UV-Vis spectroscopy using a quartz cuvette ($l = 1\text{ cm}$). Calibration curves at different conditions were performed and their correlation coefficient, from at least 5 standards, was higher than 0.9999. Approximately 0.1000 g of free film in 10 mL solutions of 0.05 M NaCl, pH = 4, pH = 10 and pH = 11.5, were used during the experiments. Solutions with the original 080 free film, under the same conditions, were used as the reference background. The aliquot was returned to the immersion solution after each measurement.

Martens microhardness was employed to obtain the hardness of the films, and the mechanical properties were assessed by tensile tests.

Electrochemical impedance spectroscopy (EIS) was used to study the performance of the coatings in terms of corrosion. The coated metallic plates were exposed to a 50 mM NaCl aqueous solution. The measurements were carried out at open circuit potential with an applied 10 mV sinusoidal perturbation in the 100 kHz to 10 mHz frequency range, taking 7 points per decade. A conventional three electrode cell was used, composed of a saturated calomel reference electrode, a platinum foil as the counter electrode, and the AA2024 substrates as the working electrodes, with a surface area of 3.35 cm^2 . The measurements were performed 2 months after the preparation of the coated substrates.

Computational study

In order to help interpret the EIS results and understand the interaction of PhPh with different aluminum surface models, density functional theory (DFT) calculations were performed using periodic expansion models of the surfaces. The calculations were performed with the Perdew–Burke–Ernzerhof (PBE) exchange correlation functional and using the semi-empirical correction of Grimme (D2) to take into account van der Waals interactions. The nuclei and core electrons were described by ultrasoft pseudopotentials, and the Kohn–Sham orbitals were expanded using planewave basis sets with 30 Ry cutoff for kinetic energy and 240 Ry cutoff for charge density, a smearing parameter of 0.02 and a $2 \times 2 \times 1$ k-point mesh. A vacuum region of 10 Å was kept between the top of the adsorbed molecule and the adjacent slab, and the Bengtsson method was used to correct the artificial electric field perpendicular to the surface.

RESULTS

Free films functionality tests

080-PhPh and 080-SiNC-PhPh free films were tested for functionality by immersion in an aqueous solution at pH = 11. After 24 h, it was possible to verify the change of color of the whole film of both samples, as can be verified in Figure 2. The change of color was found to be stronger in the case of the sample with encapsulated PhPh.

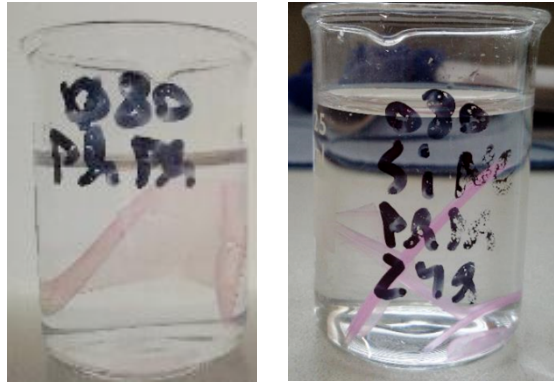


Figure 2: 080-PhPh (left) and 080-SiNC-PhPh (right) free films in an aqueous solution at pH 11 after 24 h.

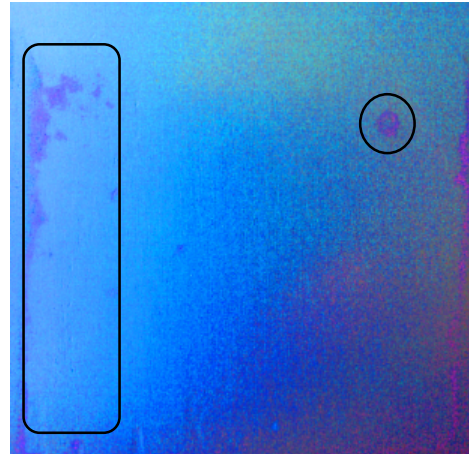
This simple experiment demonstrates the sensing potential of 080 with SiNC loaded with sensing molecules under enough aggressive conditions.

Immersion tests

Coated AA2024 plates were immersed in a 5 % NaCl solution in order to accelerate corrosion and verify if the coatings detect the associated local change of pH [3]. It was verified that only the sample with encapsulated PhPh (080-SiNC-PhPh) was able to change color and indicate the corrosion process, whereas on the case of 080-PhPh only dark spots can be noticed (Figure 3).



080-PhPh-0.3 %-9 days



080-SiNC-PhPh-3 %-9 days

Figure 3: Immersion tests in 5 % NaCl of coated AA2024 plates. In order to enhance the pink color of PhPh, the saturation of the images was increased.

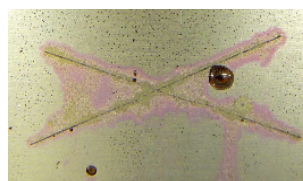
Salt-spray tests

Coated AA2024 plates were subjected to accelerated corrosion tests in a salt-spray chamber. In a small section of the plates an X scribe was done in order to analyze the response of the coatings to the accelerated corrosion process underneath.

The investigated coatings corresponded to the 080 lacquer with 3 % of dispersed SiNC-PhPh capsules and another with 0.3 % PhPh. Only 080-SiNC-PhPh was able to change color (and solely after three days of salt-spray) and indicate the corrosion process in the scribed zone. The sample with PhPh was never able to detect corrosion throughout the complete duration of the test, which lasted 17 days, which supports the need to encapsulate active compounds in order to achieve a proper coating functionality.



080-PhPh-0.3 %-3 days



080-SiNC-PhPh-3 %-3 days

Figure 4: Salt-spray tests in 5 % NaCl of coated AA2024 plates.

Reactivity of PhPh with the hardener

To obtain 080 coatings, a water-borne polyurethane emulsion is left to react with the curing agent, which contains compounds with isocyanate groups that trigger the curing process. However, there is the possibility that the hydroxyl groups of PhPh react with isocyanate groups, forming urethane units, thus explaining the deactivation of directly added PhPh.

This possibility was tested by homogenizing an equimolar mixture of PhPh and isophorone diisocyanate in tetrahydrofuran (THF) under dry atmosphere. Afterwards, the material obtained was characterized by FTIR and size exclusion chromatography (SEC). The FTIR results revealed the presence of new peaks associated with urethane bonds ($\sim 1220 \text{ cm}^{-1}$), whereas the peaks associated with isocyanate groups ($\sim 2270 \text{ cm}^{-1}$) decreased in intensity. SEC results also revealed the formation of peaks with a molecular weight typical of the formation of a polymer with approximately 7 urethane units (3839 g mol^{-1}). This experience was repeated using the hardener itself, instead of isophorone diisocyanate, and high molecular weight peaks were also obtained.

Therefore, the reactivity of PhPh towards the hardener might be one possibility to explain the deactivation of the obtained coatings when the organic compound is added directly to the formulation.

Characterization of the coatings

The obtained coatings were characterized concerning the rheology (viscosity and viscoelastic properties) of the main component of the formulation, leaching of PhPh, temperature of glass transition from DSC, thermal stability according to TGA, Martens microhardness, tensile strength, and corrosion resistance according electrochemical impedance spectroscopy (EIS). The results obtained for 080-PhPh and 080-SiNC-PhPh, in comparison with the original 080 formulation, are summarized in Table 1.

Table 1: Coating properties of 080-PhPh and 080-SiNC-PhPh in comparison with the original 080 formulation.

Property	080-PhPh	080-SiNC-PhPh
Viscosity	equal	Slightly lower than 080
Viscoelastic properties	Same pattern	Same pattern
Leaching (0.05 M NaCl, 15 days)	Not detected	Not detected
Leaching (pH = 4, 15 days)	Not detected	Not detected
Leaching (pH = 10, 15 days)	0.05 wt %	0.06 wt %
Leaching (pH = 11.5, 15 days)	0.16 wt %	0.09 wt %
Glass transition	$-(0.1 \pm 1.4) ^\circ\text{C}$	$+(0.7 \pm 1.4) ^\circ\text{C}$
Thermal stability	Lower for $T > 40 ^\circ\text{C}$	Equal for $T < 120 ^\circ\text{C}$ (lower for $T > 120 ^\circ\text{C}$)
Martens microhardness	$+(9 \pm 13) \text{ N}\cdot\text{mm}^{-2}$	$+(22 \pm 13) \text{ N}\cdot\text{mm}^{-2}$
Tensile strength	$-(4.8 \pm 4.8) \text{ MPa}$	$-(4.4 \pm 4.3) \text{ MPa}$
Corrosion resistance	Lower	Higher

In terms of rheological properties, the addition of SiNC-PhPh to the 080 formulation does not result in a detrimental interaction with the polymer. Only the viscosity becomes slightly lower than in the case of the original formulation, but this is due to the capsules being added in a water slurry form. This slightly lower viscosity also supports the good dispersion of the capsules, since large aggregates create friction when the formulation is forced to move, increasing its viscosity. Moreover, the lower viscosity still allows a good application of the film, as it is evidenced by the Martens microhardness, tensile strength and corrosion resistance, which would be affected if application was not correct.

Leaching studies of detached films in solution were also performed for 080-PhPh and 080-SiNC-PhPh under 0.05 M NaCl, pH = 4, pH = 10 and pH = 11.5. After 15 days of exposure to the solution, the leaching was not noticeable (NaCl 0.05 M and pH = 4) or happened only in very minor percentages (pH = 10 and pH = 11.5) compared to the total amount of PhPh that was added to the formulation (directly or encapsulated). The only noticeable difference between 080-PhPh and 080-SiNC-PhPh was that for very aggressive conditions (pH = 11.5), 080-PhPh leaches to a slightly greater extent than 080-SiNC-PhPh. Nevertheless, this release should only happen to areas where hydroxide anions accumulate due to the onset of corrosion.

The glass transition of 080-PhPh and 080-SiNC-PhPh is the same as the original formulation, and the thermal stability is only slightly lower in the case of 080-PhPh.

In the case of the mechanical properties, the hardness of the coating improves in the case of 080-SiNC-PhPh in comparison with the original coating, and the tensile properties for both 080-PhPh and 080-SiNC-PhPh are nearly the same within experimental uncertainty.

In terms of corrosion resistance, as studied during two months by EIS, it was obtained the following order in terms of barrier properties: 080-PhPh (worst) < 080 < 080-SiNC-PhPh (best). The worse performance of 080-PhPh can be ascribed to the detrimental interaction with the hardener or even the low solubility of PhPh in water based formulations, whereas in the

case of 080-SiNC-PhPh the good performance can be due to a positive filler effect of the capsules.

Interaction of PhPh with AA2024

In the EIS study, no active corrosion protection was verified by SiNC-PhPh. DFT periodic model calculations were used to give insight into the most favorable interaction of PhPh with aluminum surfaces, and the results were compared with the adsorption of a well-known corrosion inhibitor for aluminum alloys, 2-mercaptobenzothiazole (MBT) [11], which presents active protective functionality when SiNC-MBT [12] are applied in coatings. It was verified that the most favorable interaction of PhPh and MBT was with a bare aluminum surface, modeled by Al(111), with the molecules deprotonated and associated on the surface, as can be verified in Figure 5. The interaction energy was less favorable for PhPh than for MBT, which might contribute to explain why no active corrosion protection is verified for PhPh.

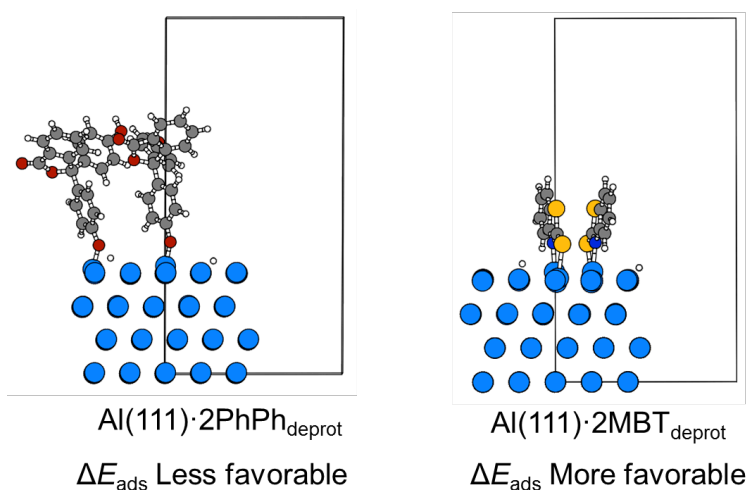


Figure 5: Adsorption mode of PhPh and MBT onto Al(111).

CONCLUSIONS

Phenolphthalein-encapsulated silica nanocapsules were used to give corrosion sensing functionality to a water borne polyurethane coating, towards aluminum alloy (AA2024). SiNC-PhPh performed better than the direct addition of PhPh to the formulation, according to immersion tests of the free films, and immersion and salt-spray standard tests of the coated metallic plates.

It was demonstrated that the reason for the failure of directly added PhPh to detect corrosion was due to a detrimental reaction of PhPh with the hardener.

The new formulation with SiNC-PhPh performed in agreement with the original formulation or without any obstacle to its application, according to rheological properties, leaching studies, glass transition, thermal stability, leaching of active compound, hardness and mechanical properties, while having improved barrier properties.

The conclusions obtained in this study are transferable to other types of functional coatings, namely self-healing [13] and anti-fouling [14] coatings, where nanocontainers are also employed.

ACKNOWLEDGEMENTS

This work was developed in the scope of the project CICECO – Aveiro Institute of Materials, POCI-01-0145-FEDER-007679 (Ref. FCT UID/CTM/50011/2013), financed by national funds through the FCT/MEC and when applicable co-financed by FEDER under the PT2020 Partnership Agreement. This work has received funding from the European Union's Horizon 2020 research and innovation programme under the Marie Skłodowska-Curie grant agreements No 645662. It was also financed in the framework of the project reference PTDC/QEQ-QFI/4719/2014, Project 3599 - Promover a Produção Científica e Desenvolvimento Tecnológico e a Constituição de Redes Temáticas (3599-PPCDT) and FEDER funds through COMPETE 2020, Programa Operacional Competitividade e Internacionalização (POCI). The authors also thank financial support from FCT and COMPETE (Programa Investigador FCT). JT thanks FCT for the research grant IF/00347/2013.

REFERENCES

1. J. Zhang, G. S. Frankel, "Corrosion-Sensing Behavior of an Acrylic-Based Coating System," *Corrosion*, 55 (1999): p 957.
2. I. M. El-Nahhal, S. M. Zourab, N. M. El-Ashgar, "Encapsulation of phenolphthalein pH-indicator into a sol-gel matrix," *J. Dispersion Sci. Technol.*, 22 (2001): p. 583.
3. W. Li, L. M. Calle, "Controlled release microcapsules for smart coatings," *NACE Corrosion 2007*, Paper 07228 (Nashville, TN).
4. A. C. Bastos, O. V. Karavai, M. L. Zheludkevich, K. A. Yasakau, M. G. S. Ferreira, "Localised Measurements of pH and Dissolved Oxygen as Complements to SVET in the Investigation of Corrosion at Defects in Coated Aluminum Alloy," *Electroanalysis*, 22 (2010): p 2009.
5. F. Maia, J. Tedim, A. C. Bastos, M. G. S. Ferreira, and M. L. Zheludkevich, "Active sensing coating for early detection of corrosion processes," *RSC Adv.*, 4 (2014): p. 17780.
6. K. Qian, T. Shi, S. He, L. Luo, X. liu, Y. Cao, "Release kinetics of tebuconazole from porous hollow silica nanospheres prepared by miniemulsion method," *Microporous Mesoporous Mater.*, 169 (2013): p. 1.
7. I. Sousa, F. Maia, A. Silva, Â. Cunha, A. Almeida, D. V. Evtugin, J. Tedim, M. G. Ferreira, "A novel approach for immobilization of polyhexamethylene biguanide within silica capsules," *RSC Adv.*, 5 (2015): p. 92656.
8. K. Qian, T. Shi, S. He, L. Luo, X. liu, Y. Cao, "Release kinetics of tebuconazole from porous hollow silica nanospheres prepared by miniemulsion method," *Microporous Mesoporous Mater.*, 169 (2013): p. 1.
9. I. Sousa, F. Maia, A. Silva, Â. Cunha, A. Almeida, D. V. Evtugin, J. Tedim, M. G. Ferreira, "A novel approach for immobilization of polyhexamethylene biguanide within silica capsules," *RSC Adv.*, 5 (2015): p. 92656.
10. F. Maia, J. Tedim, A.C. Bastos, M.G.S. Ferreira, M.L. Zheludkevich, "Nanocontainer-based corrosion sensing coating," *Nanotechnology*, 24, 41 (2013): p. 415502.
11. T.G. Harvey, S.G. Hardin, A.E. Hughes, T.H. Muster, P.A. White, T.A. Markley, et al., "The effect of inhibitor structure on the corrosion of AA2024 and AA7075," *Corros. Sci.*, 53 (2011), p. 2184.
12. F. Maia, J. Tedim, A. D. Lisenkov, A. N. Salak, M. L. Zheludkevich, M. G. S. Ferreira, "Silica nanocontainers for active corrosion protection," *Nanoscale*, 4 (2012), p. 1287.
13. J. Tedim, S.K. Poznyak, A. Kuznetsova, D. Raps, T. Hack, M.L. Zheludkevich, et al., "Enhancement of Active Corrosion Protection via Combination of Inhibitor-Loaded Nanocontainers," *ACS Appl. Mater. Interfaces*, 2 (2010), p. 1528.
14. F. Maia, A.P. Silva, S. Fernandes, A. Cunha, A. Almeida, J. Tedim, et al., "Incorporation of biocides in nanocapsules for protective coatings used in maritime applications," *Chem. Eng. J.*, 270 (2015), p. 150.